PHYSICAL REVIEW E **91**, 030501(R) (2015)

Topological defect transformation and structural transition of two-dimensional colloidal crystals across the nematic to smectic-*A* phase transition

K. P. Zuhail,[1] P. Sathyanarayana,[1] D. Seč,[2,3] S. Čopar,[2,3] M. Škarabot,[3] I. Muševič,[2,3] and S. Dhara[1,*]

[1]*School of Physics, University of Hyderabad, Hyderabad-500046, India*

[2]*J. Stefan Institute, Jamova 39, SI-1000 Ljubljana, Slovenia*

[3]*Faculty of Mathematics and Physics, University of Ljubljana, Jadranska 19, SI-1000 Ljubljana, Slovenia*

(Received 22 April 2014; revised manuscript received 21 November 2014; published 10 March 2015)

We observe that topological defects in nematic colloids are strongly influenced by the elasticity and onset of smectic layering across the nematic (N) to smectic-A (SmA) phase transition. When approaching the SmA phase from above, the nematic hyperbolic hedgehog defect that accompanies a spherical colloidal inclusion is transformed into a focal conic line in the SmA phase. This phase transformation has a strong influence on the pairwise colloidal interaction and is responsible for a structural transition of two-dimensional colloidal crystals. The pretransitional behavior of the point defect is supported by Landau–de Gennes Q-tensor modeling accounting for the increasing elastic anisotropy.

DOI: 10.1103/PhysRevE.91.030501 PACS number(s): 61.30.Jf, 82.70.Dd

Topological defects [1,2] are point-, string-, wall-, or looplike singularities of physical fields that are studied in very different systems, such as the early Universe or condensed matter. In condensed matter, topological defects are observed as vortices in superfluid helium [3], Abrikosov vortices in type-II superconductors [4], domain walls in soft ferromagnets [5], etc. In liquid crystals, topological defects are generated by the symmetry breaking phase transition from the isotropic to the liquid crystalline phase [6]. They can also be produced and manipulated in a controlled way by introducing foreign particles into the uniformly aligned liquid crystal [7,8]. For example, microspheres with perpendicular (homeotropic) surface alignment of nematic liquid crystal (NLC) molecules are accompanied by topological point defects, thus forming elastic dipoles in the bulk NLC. Depending on the anchoring strength and confinement, defects may also appear in the form of Saturn rings and boojums [9]. Due to elastic distortion of the NLC around each particle, nematic colloids experience long range forces [10], which opens new directions in colloidal assembly. There are many theoretical and experimental studies of topological defects and colloidal interactions in the NLCs [10–16], mainly motivated by fascinating self-assembled colloidal superstructures, such as chains [7], two- [8] and three-dimensional crystals [11], entangled clusters [13,17,18], knotted and linked particles [19–22], and chiral nematic colloids [23,24].

However, little is known about the behavior of topological defects and colloidal structures when crossing the phase transition point, such as the N-SmA phase transition. In this Rapid Communication, we study the transformation of a topological defect across the N-SmA phase transition, where, in addition to the long range orientational order of NLC molecules, a one-dimensional positional order of NLC molecules is established and results in smectic layering on the nanoscale. We observe a structural transition in a two-dimensional (2D) dipolar colloidal crystal, where defect transformation, interparticle separation, and lattice rearrangement are governed by the elasticity of the nematic and SmA phases.

In experiments, we used silica microspheres, coated with DMOAP [octadecyldimethyl (3-trimethoxysilylpropyl) ammonium chloride] to obtain perpendicular (homeotropic) alignment of LC molecules on the surface [8]. The microspheres were dispersed in 8CB (4′-*n*-octyl-4-cyano-biphenyl) liquid crystal. 8CB exhibits the following phase transitions: Cr (crystal) 21.5 °C SmA (smectic-A), 33.5 °C N (nematic), 40.5 °C I (isotropic), and a positive elastic anisotropy, i.e., $\Delta K = K_{33} - K_{11} > 0$, where K_{33} and K_{11} are the bend and splay elastic constants. The experimental details and additional measurements are stated in the Supplemental Material (SM) [25].

Figures 1(a), 1(c), and 1(e) show the transformation of a hyperbolic point defect, associated with an isolated microsphere, across the N-SmA phase transition in a thick planar cell (15 μm). One can clearly see three stages in the transformation of a point defect in the N phase into a line defect in the SmA phase. As the temperature is decreased from the nematic into the SmA phase, a point defect in the nematic 8CB LC is forced to move towards the microsphere's surface [compare Figs. 1(a) and 1(c)], and a high-contrast "tail" emanates from the point defect. To confirm that the elastic constant anisotropy is the main contributor to the transformations seen in the experiment, this effect was qualitatively reproduced by Landau–de Gennes Q-tensor modeling [26,27] of the N phase. Lowering the temperature increases the K_{33} (bend) elastic constant relative to K_{11} (splay). Figures 1(b) and 1(d) show simulated optical transmission micrographs between crossed polarizers for two elastic constant ratios in the N phase. The increase of K_{33} [Figs. 1(c) and 1(d)] replaces the energetically costly bend distortions around the particle by more favorable splay distortions, concentrated in an elongated tail, forming a sort of a "splay soliton." A video (Video-1) of topological defect transformation across the N-SmA transition and the details of the simulation are given in the SM [25].

In the SmA phase we observe a long and dark tail-like structure in place of the splay soliton seen already in the N phase [Fig. 1(e)]. To find the molecular orientation in the tail, we used a full wave retardation plate (530 nm) between the analyzer and the sample as is explained in the SM. This method helped us to reconstruct an approximate

*sdsp@uohyd.ernet.in

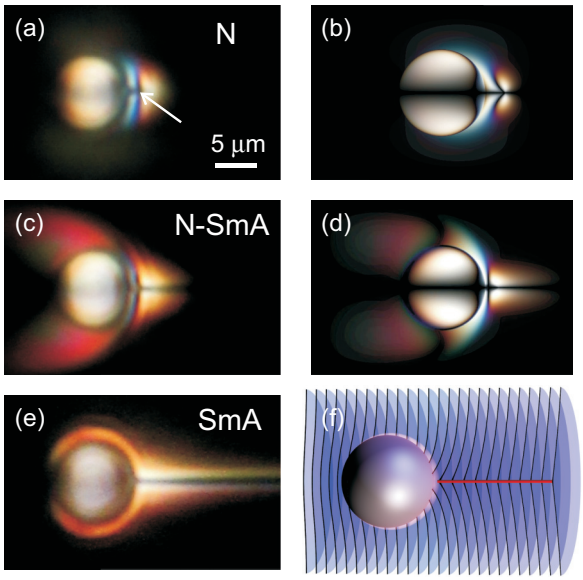

FIG. 1. (Color online) (a),(c),(e) Experimental optical micrographs of 7 μm homeotropic microspheres in a thick planar 8CB cell between crossed polarizers in the nematic phase, (a) just before the N-SmA transition (c) and after the transition (e). Cell thickness is 15 μm. The hyperbolic hedgehog defect in the nematic phase is marked with an arrow (a). (b), (d) Simulated micrographs of the N phase for (b) equal Frank elastic constants $K_{33} = K_{11}$ and for (d) increased bend elastic constant ($K_{33} = 8K_{11}$) which pushes the hedgehog towards the particle's surface. (f) The sketch of a reconstructed cross section of smectic layer structure in the vicinity of the microsphere.

geometry of the layer structure, as shown schematically in Fig. 1(f). The requirement for equally spaced layers in the SmA phase geometrically constrains the preexisting nematic order; because the splay soliton in the form seen in the N phase does not allow smooth equidistant layers, the tail is forced into a focal line with the cusp angle in the layer shape that falls off slowly with the distance from the particle [Figs. 1(e) and 1(f)]. The layer incompressibility further decreases the range of influence of the boundary conditions imposed by the particle. The homeotropic boundary condition is reconciled in a zone next to the microsphere surface, too narrow to be discerned optically. Outside this energetically costly boundary zone, the layers are only moderately bent compared to the far field. On the defect-adjacent hemisphere, the layers outside the boundary zone closely resemble the configuration for the planar surface anchoring [28], while the opposite hemisphere obeys the homeotropic anchoring and the boundary zone is not needed. The particle effectively "lenses" the layers into a cusp, similar to the effect of curvature in 2D smectic structures [29].

Because the elasticity and smectic layering have such a strong influence on topological defects, we expect that the forces between colloidal particles should be strongly influenced by the N-SmA transition as well. We first investigate a pair of particles, which spontaneously chain together in the N phase, as shown in the right-hand inset in Fig. 2(a). The microspheres attract via the elastic deformation of the NLC but are separated by a topologically required hedgehog point defect in between, which stabilizes the structure. The

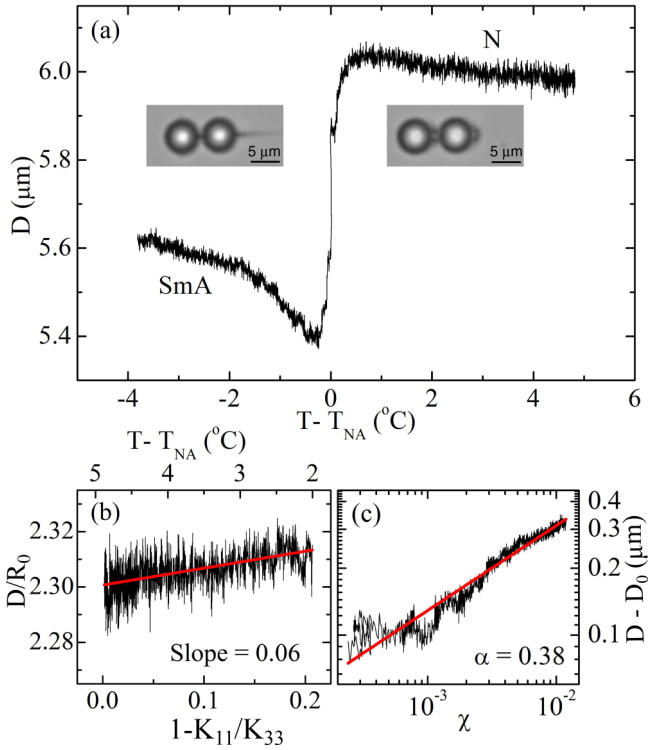

FIG. 2. (Color online) (a) Variation of the center to center separation (D) of two homeotropic microspheres across the N-SmA transition in 8CB. See SM (Video-2). The microsphere diameter is 5.2 μm, and the cell thickness is 7.7 μm. Insets show experimental images of a pair of dipolar microspheres before and after N-SmA transition. (b) Variation of D/R_0 above the N-SmA transition as a function of the elastic constant anisotropy ($1 - K_{11}/K_{33}$). The red line is the best fit to Eq. (1) with a slope 0.06. The scale on the top shows the temperature range that corresponds to the anisotropy range on the principal axis. (c) Variation of the separation with reduced temperature below the transition (logarithmic scale). The red line shows the best fit to the power law $(D - D_0) \sim |\chi|^{\alpha}$ with $\alpha = 0.38$.

equilibrium separation of the pair is governed by the nematic elasticity and should therefore be highly sensitive to the onset of N-SmA phase transition.

Figure 2(a) shows the temperature dependence of microsphere separation (D) across the N-SmA transition. We see that D increases with decreasing temperature in the N phase, which is followed by a sharp jump at the N-SmA phase transition. In 8CB, we find 5 °C above the N-SmA transition, $D = 2.3R_0$, which is close to the previous reports [30–32]. Recently, James *et al.* theoretically studied the effect of anchoring strength and elastic anisotropy on the separation of a pair of dipolar nematic colloids [33]. In 8CB, considering $R_0 = 2.6\,\mu$m, the anchoring strength $W \simeq 10^{-4}$ J/m^2, and the bend elastic constant around $K_{33} = 10$ pN, we get $K_{33}/WR_0 \leqslant 0.04$, which is in the limit of strong surface anchoring, justifying the approximation for the equilibrium separation (D) with a linear relation

$$D/R_0 \simeq 2.439 + 0.0878(1 - K_{11}/K_{33}). \qquad (1)$$

In order to verify that, we collected the temperature dependencies of K_{11} and K_{33} for 8CB from Ref. [34] and

interpolated for all temperatures of interest. Since K_{33} depends on temperature, we selected an appropriate temperature range (considering the size of the microsphere) in which the assumption of strong anchoring is valid. Figure 2(b) shows the variation of D/R_0 as a function of elastic anisotropy $(1 - K_{11}/K_{33})$ with the best fit to Eq. (1). The experimentally measured slope of D/R_0 for 5.2 μm particles is 0.06, which is slightly lower than the predicted value. In the selected regime, the anisotropy is small and the linearity holds. Closer to the transition, an increase of K_{33} makes the surface anchoring comparatively small, which is another explanation for why the hedgehog can move closer to the surface.

The N-SmA phase transition is reflected in a rather sharp discontinuity of the interparticle separation D, marking the discontinuity of the elastic constants and the onset of smectic layering. Furthermore, in the SmA phase [Fig. 2(a)], D is increasing with decreasing temperature from the N-SmA transition point and tends to saturate at lower temperatures. This indicates that the layer compressibility is important, because it is known that in the SmA phase, the layer compression elastic modulus (B) varies as $B \sim \chi^{\alpha}$, where $\chi \equiv (1 - T/T_{NA})$ is the reduced temperature, and the critical exponent α is between 0.39 and 0.42. To identify the role of the layer compression modulus, we fitted the temperature variation of separation to $(D - D_0) \sim \chi^{\alpha}$, where D_0 is the minimum value just below the transition. As shown in Fig. 2(c), the best fit gives critical exponent $\alpha = 0.38$. This is in the range (0.36–0.38) of reported values measured by a second-sound resonance technique [35]. To confirm the generality of our findings, we studied particles with different size in 8CB and also in a different liquid crystal, namely, 4′-butyl-4-heptyl-bicyclohexyl-4-carbonitrile (CCN-47). It may be mentioned that CCN-47 exhibits a negative elastic anisotropy ($\Delta K < 0$). The results are presented in the SM (also see Video-3) [25].

Finally we show the effect of N-SmA phase transition on the 2D dipolar colloidal crystal, assembled by laser tweezers. The crystal was prepared following the procedure reported in Ref. [8]. Figure 3(a) shows a 2D dipolar crystal made of 64 assembled microspheres with diameter 5.2 μm in the nematic. Figure 3(b) shows the image of a 2D crystal in the SmA phase and it was obtained by cooling the sample from the nematic phase at a rate of 0.3 °C/min. The corresponding images under crossed polarizers are given in the SM. In the nematic phase it shows an oblique lattice with lattice constants $a = 6.18 \pm 0.05$ μm ($\simeq 2.38R_0$), $b = 6.51 \pm 0.05$ μm ($\simeq 2.5R_0$), and $\gamma = 61^{\circ} \pm 1^{\circ}$, which are comparable to those reported by Muševič *et al.* [8] in 5CB (4-cyano-4′-pentylbiphenyl) NLC. As the temperature is reduced towards the SmA phase, the crystal expands in a direction perpendicular to the chains and the point defects are transformed into focal conic lines at the transition; consequently, the crystal collapses into a hexagonal structure in the SmA phase (see SM Video-4) [25]. The transition is reversible in the sense that the 2D dipolar crystal is almost restored and the hyperbolic hedge defects reappear at the same places when the sample is again heated back to the nematic phase (see SM Video-5) [25]. Careful observation indicates that in the SmA phase, the microspheres are slightly displaced from the common plane (~1 μm) in an alternating striped pattern. This suggests that it is more favorable to buckle the crystal into the third dimension, which

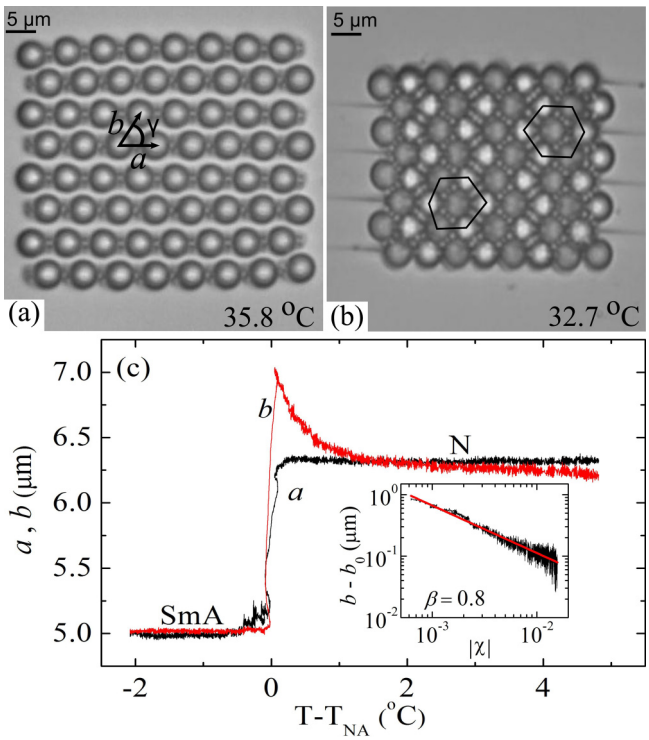

FIG. 3. (Color online) Optical photomicrograph of a 2D dipolar crystal of particles with diameter 5.2 μm in the N phase (35.8 °C) and SmA phase (32.7 °C) of 8CB. (a),(b) Between crossed polarizers; (c),(d) without polarizers. See SM video-4. (e) Temperature variation of the lattice parameters a and b across the N-SmA transition. Inset: Temperature variation of b with the best fit (red line) to $b = b_0 + C|\chi|^{-\beta}$ with $\beta = 0.8$ (logarithmic scale). Diameter of the microspheres is 5.2 μm and cell thickness is 9.3 μm.

will play a more important role in thicker cells. The area of the 2D crystal decreases from 2400 (nematic phase) to 1560 μm^2 (SmA phase) which is about a 35% reduction of the initial crystal area. This is due to the absence of hedgehog point defects and out of plane shift of some particles. Using a particle tracking method, we measured the temperature dependence of the lattice constants, shown as a and b in Fig. 3(c). Interestingly, the lattice parameter a (measuring the separation along the chain) remains nearly constant, while b exhibits the presmectic divergence and finally both jump to a smaller value in the SmA phase. We also measured the angle γ [Fig. 3(a)] and no noticeable change is observed across the phase transition. In the N phase there is a strong bend deformation of the director between the neighboring chains [8]. This bend deformation is expected to get expelled due to the pretransitional divergence of the bend elastic constant, which is given by $K_{33} = K_{33}^0 + A|\chi|^{-1}$ [36]. In order to identify the role of bend deformation, the temperature dependence of b is fitted to $b = b_0 + C|\chi|^{-\beta}$, where b_0 and C are constants. The fit [inset of Fig. 3(c)] gives the exponent $\beta \simeq 0.8$, close to the theoretical exponent of pre-smectic bend elastic constant and suggests that the divergent behavior of b, consequently the anisotropic crystal expansion is due to the expulsion of bend deformation. Further, we studied the structural transition in CCN-47 on both cooling and heating (Video-6 and Video-7 in SM) [25]. The structural transition and

the temperature dependence of lattice parameters are almost similar to that observed in 8CB. The experimental results are presented in the SM. This suggests that the structural transition of the 2D dipolar crystal across the N-SmA phase transition is driven by transformation of topological defects and controlled by the elasticity of the respective media.

In conclusion, we observed the transformation of the hyperbolic hedgehog point defect into a focal conic line across the N-SmA phase transition. This transformation is due to the N-SmA pretransitional divergence of the bend elastic constant and the emergence of smectic layering. It strongly affects not only pair colloidal interactions, but has a profound effect on the restructuring of 2D colloidal crystals across the N-SmA phase transition. We believe this study of transformation of topological defects across the phase transition will initiate new theoretical and experimental investigations on the topology and phase transitions in soft matter.

S.D. acknowledges the support from DST-PURSE and UPE-II. K.P.Z. acknowledges UGC for support through a fellowship. I.M., S.Č., and D.S. acknowledge Slovenian Research Agency (ARRS) for support under Contracts No. J1-6723 (D.S.) and No. Z1-6725 (S.Č.). D.S. also acknowledges funding by EU MC program FREEFLUID. We thank Prof. Slobodan Žumer for useful discussions.

[1] N. D. Mermin, Rev. Mod. Phys. **51**, 591 (1979).
[2] P. M. Chaikin and T. C. Lubensky, *Principles of Condensed Matter Physics* (Cambridge University Press, Cambridge, UK, 1995).
[3] N. D. Mermin and Tin-Lun Ho, Phys. Rev. Lett. **36**, 594 (1976).
[4] D. J. Bishop, P. L. Gammel, D. A. Huse, and C. A. Murray, Science **255**, 165 (1992).
[5] O. Tchernyshyov and Gia-Wei Chern, Phys. Rev. Lett. **95**, 197204 (2005).
[6] I. Chuang, R. Durrer, N. Turok, and B. Yurke, Science **251**, 1336 (1991).
[7] P. Poulin, H. Stark, T. C. Lubensky, and D. A. Weitz, Science **275**, 1770 (1997).
[8] I. Muševič, M. Škarabot, U. Tkalec, M. Ravnik, and S. Žumer, Science **313**, 954 (2006).
[9] H. Stark, Phys. Rep. **351**, 387 (2001).
[10] T. C. Lubensky, D. Pettey, N. Currier, and H. Stark, Phys. Rev. E **57**, 610 (1998).
[11] A. Nych, U. Ognysta, M. Škarabot, M. Ravnik, S. Žumer, and I. Muševič, Nat. Commun. **4**, 1489 (2013).
[12] O. Guzmán, E. B. Kim, S. Grollau, N. L. Abbott, and J. J. de Pablo, Phys. Rev. Lett. **91**, 235507 (2003).
[13] M. Ravnik, M. Škarabot, S. Žumer, U. Tkalec, I. Poberaj, D. Babič, N. Osterman, and I. Muševič, Phys. Rev. Lett. **99**, 247801 (2007).
[14] M. Vilfan, N. Osterman, M. Čopič, M. Ravnik, S. Žumer, J. Kotar, D. Babič, and I. Poberaj, Phys. Rev. Lett. **101**, 237801 (2008).
[15] I. I. Smalyukh, O. D. Lavrentovich, A. N. Kuzmin, A. V. Kachynski, and P. N. Prasad, Phys. Rev. Lett. **95**, 157801 (2005).
[16] T. A. Wood, J. S. Lintuvuori, and A. B. Schofield, Science **333**, 79 (2011).
[17] M. Zapotocky, L. Ramos, P. Poulin, T. C. Lubensky, and D. A. Weitz, Science **283**, 209 (1999).
[18] T. Araki and H. Tanaka, Phys. Rev. Lett. **97**, 127801 (2006).
[19] U. Tkalec, M. Ravnik, S. Čopar, S. Žumer, and I. Muševič, Science **333**, 62 (2011).
[20] V. S. R. Jampani, M. Škarabot, M. Ravnik, S. Čopar, S. Žumer, and I. Muševič, Phys. Rev. E **84**, 031703 (2011).
[21] B. Senyuk, Q. Liu, S. He, R. D. Kamien, R. B. Kusner, T. C. Lubensky, and I. I. Smalyukh, Nature (London) **493**, 200 (2013).
[22] T. Machon and G. P. Alexander, Proc. Natl. Acad. Sci. USA **110**, 14174 (2013).
[23] V. S. R. Jampani, M. Škarabot, S. Čopar, S. Žumer, and I. Muševič, Phys. Rev. Lett. **110**, 177801 (2013).
[24] J. S. Lintuvuori, K. Stratford, M. E. Cates, and D. Marenduzzo, Phys. Rev. Lett. **105**, 178302 (2010).
[25] See Supplemental Material at http://link.aps.org/supplemental/10.1103/PhysRevE.91.030501 for experimental details, additional measurements, effect of particle size, and several video clips across the phase transition.
[26] M. Ravnik and S. Žumer, Liq. Cryst. **36**, 1201 (2009).
[27] C. Blanc, D. Svenšek, S. Žumer, and M. Nobili, Phys. Rev. Lett. **95**, 097802 (2005).
[28] C. Blanc and M. Kleman, Eur. Phys. J. E **4**, 241 (2001).
[29] R. A. Mosna, D. A. Beller, and R. D. Kamien, Phys. Rev. E **86**, 011707 (2012).
[30] J.-i. Fukuda, H. Stark, M. Yoneya, and H. Yokoyama, Phys. Rev. E **69**, 041706 (2004).
[31] P. Poulin and D. A. Weitz, Phys. Rev. E **57**, 626 (1998).
[32] C. M. Noel, G. Bossis, A. M. Chaze, F. Giulieri, and S. Lacis, Phys. Rev. Lett. **96**, 217801 (2006).
[33] R. James and J.-i. Fukuda, Phys. Rev. E **88**, 010501(R) (2013).
[34] S. Morris, P. P. Muhoray, and D. A. Balzarini, Mol. Cryst. Liq. Cryst. **139**, 263 (1986).
[35] M. Benzekri, J. P. Marcerou, H. T. Nguyen, and J. C. Rouillon, Phys. Rev. B **41**, 9032 (1990).
[36] P. G. de Gennes, Mol. Cryst. Liq. Cryst. **21**, 49 (1973).